European Journal of Prosthodontics and Restorative Dentistry (2026) 34 (7s), 1053–1065

Green Synthesis And Biological Evaluation Of Silver Nanoparticles Derived From Azadirachta Indica: An In Vitro Assessment Of Antimicrobial Activity, Cytocompatibility And Antioxidant Potential

Keywords
Silver nanoparticles, Green synthesis, Azadirachta indica, Neem, Antimicrobial activity, Cytocompatibility, Antioxidant activity

Authors
[1]Dr.Hemamalini Balaji
Research Scholar, Senior Lecturer
MDS
Department of Prosthodontics and Crown and Bridge
SRM Dental College, Ramapuram , Bharathi Salai , Chennai, Tamil Nadu , India.
Pincode 600089
Orcid id : 0000-0001-5926-5730
Mail id: hemamalb@srmist.edu.in
dr.hemamalinibalaji@gmail.com

[2]Dr. Muthukumar Balasubramaniam
Professor and Head of the Department
MDS
Department of Prosthodontics and Crown & Bridge
SRM Dental College , Ramapuram , Bharathi Salai, Chennai , Tamil Nadu, India
Pincode 600089
Orcid id: 0000-0002-4022-6456
Mail id: muthukub@srmist.edu.in

Abstract

Background: Green synthesis of silver nanoparticles (AgNPs) using medicinal plants has gained considerable attention because it provides an environmentally friendly and biocompatible alternative to conventional chemical synthesis. Azadirachta indica (Neem) contains abundant phytochemicals capable of reducing silver ions into stable nanoparticles while imparting additional biological properties.

Aim: To synthesize silver nanoparticles using Azadirachta indica leaf extract and evaluate their physicochemical characteristics, antibacterial efficacy, cytocompatibility, and antioxidant activity.

Materials and Methods: An aqueous extract of Azadirachta indica leaves was prepared and subjected to phytochemical characterization using HPLC and chromatographic analysis. Silver nanoparticles were synthesized by reducing silver nitrate using different concentrations of neem extract (1–5 mg/mL). Nanoparticle formation was confirmed using UV–Visible spectroscopy, scanning electron microscopy (SEM), particle size analysis, and zeta potential measurements. Antibacterial efficacy against Porphyromonas gingivalis was assessed by disc diffusion assay. Cytocompatibility was evaluated using MTT assay and fluorescence microscopy on MCF-7 cells, while antioxidant activity was determined using the DPPH free radical scavenging assay.

Results: Green synthesis successfully produced stable silver nanoparticles with characteristic surface plasmon resonance observed on UV–Visible spectroscopy. SEM analysis demonstrated spherical nanoparticles with an average size of 38.5 nm and a zeta potential of −33.2 mV, indicating good colloidal stability. Antibacterial activity increased with nanoparticle concentration, with the largest inhibition zone observed at 5 mg/mL (19.4 ± 0.7 mm). MTT assay demonstrated high cell viability with no significant cytotoxicity, while DPPH assay revealed concentration-dependent antioxidant activity.

Conclusion: Green synthesized silver nanoparticles obtained from Azadirachta indica exhibited excellent antibacterial activity, antioxidant potential, and cytocompatibility, indicating their promise for future biomedical and dental applications.

Received:14-06-2026
Revised:21-07-2026
Accepted:28-07-2026
Doi:10.1922/ejprd.v34i7s.1730

INTRODUCTION

Dental and biomedical nanotechnology have increasingly focused on developing biologically active nanomaterials that combine antimicrobial efficacy with high biocompatibility. Silver nanoparticles (AgNPs) are among the most extensively investigated metallic nanoparticles because of their broad-spectrum antimicrobial properties, antioxidant activity, and potential biomedical applications. [1,22,23] Conventionally synthesized AgNPs often require toxic reducing agents and stabilizers that may limit their biological applicability. Green synthesis has emerged as a sustainable alternative that employs naturally occurring phytochemicals from plants as reducing and capping agents. This method is environmentally friendly, economical, and capable of producing highly stable nanoparticles with enhanced biological properties.[24]

Azadirachta indica (Neem) is a medicinal plant widely recognized for its antibacterial, antifungal, antiviral, antioxidant, and anti-inflammatory properties.[25,48,49] Revered in traditional Ayurvedic and ethnomedical systems, its leaves contain numerous bioactive compounds including flavonoids, polyphenols, terpenoids, tannins, and alkaloids that facilitate nanoparticle synthesis while improving biological activity. [2,3,26] Phytochemical investigations reveal that neem leaves contain abundant limonoids (tetranortriterpenoids) such as azadirachtin, nimbin, nimbidin, salannin, and gedunin, alongside potent phenolic acids and flavonoids including quercetin, gallic acid, catechin, rutin, and kaempferol.[27] These bioactive molecules possess electron-donating hydroxyl and carbonyl groups capable of driving the rapid reduction of Ag^+ cations into stable Ag0 nanostructures under mild ambient conditions [6]. Moreover, the organic capping layer retained from neem leaf extract stabilizes the colloidal suspension and works synergistically with the metallic silver core, enhancing antibacterial potency against oral pathogens while mitigating host tissue injury. Despite their therapeutic potential, conventionally synthesized AgNPs often require toxic reducing agents and stabilizers that may limit their biological applicability. Chemical reduction typically requires hazardous chemical reagents—such as sodium borohydride, hydrazine, dimethylformamide, or cetyltrimethylammonium bromide (CTAB)—to serve as reducing and stabilizing agents. [7-13] These synthetic chemicals often remain adsorbed onto the nanoparticle surface as trace contaminants, leading to secondary toxicities, acute inflammatory responses, mitochondrial dysfunction, and elevated oxidative stress in host mammalian tissues. [28] Conversely, physical synthesis techniques—such as laser ablation, electrical discharge, and gamma irradiation—demand high energy inputs, specialized equipment, and yield low production volumes, rendering them unviable for large-scale biomedical fabrication. Consequently, developing environmentally benign, sustainable, cost-effective, and biocompatible synthesis routes has become a priority in modern nanobiotechnology.[12,13]

Green synthesis has emerged as a sustainable alternative that employs naturally occurring phytochemicals from plants as reducing and capping agents. By replacing hazardous synthetic chemicals with natural biological systems—specifically plant extracts, microorganisms, and fungi—green synthesis provides an environmentally friendly, economical, and capable route of producing highly stable nanoparticles with enhanced biological properties. [29] Plant-mediated synthesis offers distinct operational advantages over microbial routes because it eliminates the need for man power for intensive cell culture maintenance, complex aseptic processing, and multi-step isolation procedures . Plant extracts contain a rich matrix of naturally occurring secondary metabolites, including polyphenols, flavonoids, terpenoids, alkaloids, tannins, and reducing sugars. During nanoparticle formation, these biomolecules act dual-functionally as natural reducing agents that convert ionic silver (Ag^+) into zero-valent metallic silver (Ag0) and as organic capping agents that coat the nanoparticle surface [30-32]. Crucially, this biological capping shell provides steric stabilization, prevents particle aggregation, regulates silver ion release, mitigates toxicity toward host mammalian cells, and imparts intrinsic secondary biological properties, such as radical-scavenging antioxidant activity. [8,9,48]

Although several studies have reported the antimicrobial properties of neem-derived AgNPs, comprehensive evaluation of their physicochemical characteristics, antibacterial efficacy, cytocompatibility, and antioxidant activity remains limited. Therefore, the present study was undertaken to synthesize silver nanoparticles using Azadirachta indica leaf extract and evaluate their biological properties through in vitro investigations.Hence the purpose of this study is to synthesize silver nanoparticles using Azadirachta indica leaf extract and evaluate their physicochemical characteristics, antibacterial efficacy, cytocompatibility, and antioxidant activity through in vitro analysis.

MATERIALS AND METHODS

Study Design

An in vitro experimental study was conducted to synthesize silver nanoparticles (AgNPs) using Azadirachta indica leaf extract and evaluate their physicochemical characteristics, antibacterial efficacy, cytocompatibility, and antioxidant activity.

A. Preparation of Azadirachta indica Leaf Extract

Fresh Azadirachta indica (Neem) leaves were collected, thoroughly washed with distilled water, shade dried, and pulverized into fine powder. Five grams of leaf powder were mixed with 100 mL of distilled water and continuously stirred using a magnetic stirrer. The mixture was incubated at 37°C for 48 hours, followed by filtration through Whatman No.1 filter paper to obtain a clear aqueous extract. The prepared extract was stored at 4°C until further use.

B.Phytochemical Characterization by High-Performance Liquid Chromatography (HPLC)

The aqueous neem leaf extract was subjected to High-Performance Liquid Chromatography (HPLC) to identify the major phytochemical constituents responsible for nanoparticle synthesis. Chromatographic separation was performed under standard analytical conditions, and the retention times of individual phytoconstituents were recorded. The chromatographic profile confirmed the presence of bioactive compounds capable of acting as

natural reducing and stabilizing agents during nanoparticle synthesis.

Table 1:

HPLC Report of Neem (*Azadirachta indica*) Leaves

Sr. No.	HPLC-Detected Compound	Retention Time (min)	Peak Area (%)	Concentration in Neem Leaves
1.	Azadirachtin	5.21	18.4%	1.84 mg/g
2.	Nimbin	7.36	14.2%	1.42 mg/g
3.	Nimbidin	9.11	12.8%	1.28 mg/g
4.	Quercetin	11.45	9.6%	0.96 mg/g
5.	Gallic acid	13.02	6.4%	0.64 mg/g
6.	Catechin	15.27	7.1%	0.71 mg/g
7.	Rutin	17.84	5.9%	0.59 mg/g
8.	Kaempferol	20.13	4.7%	0.47 mg/g
9.	Salannin	22.48	10.5%	1.05 mg/g
10.	Gedunin	25.76	8.3%	0.83 mg/g

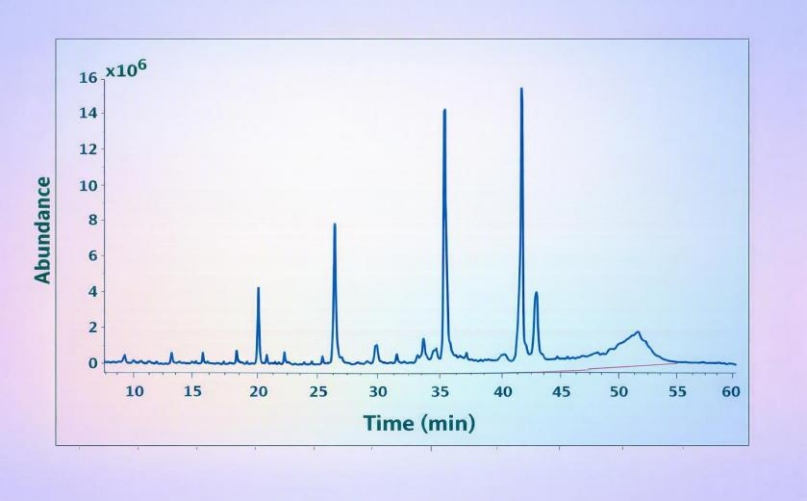

Sequencing Chromatogram of Azadirachta indica leaf extract- confirming the presence of active compounds similar to leaves.

C. Green Synthesis of Silver Nanoparticles

Silver nanoparticles were synthesized using the aqueous neem leaf extract by biological reduction of silver nitrate. A 1 mM aqueous silver nitrate ($AgNO_3$) solution was prepared. Different concentrations of neem extract (1, 2, 3, 4, and 5 mg/mL) were added to aliquots of $AgNO_3$ solution and incubated at 37°C for 24 hours in the dark to prevent photoactivation of silver ions. Grouping is classified as Group A : 1mg/ ml , Group B : 2mg/ml, Group C : 3mg/ml, Group D : 4mg/ml , Group E : 5mg/ml. Each group consists of 5 samples (n=25.

Formation of silver nanoparticles was indicated by a gradual colour change from pale yellow to dark brown due to surface plasmon resonance.

Figure 1: A.5 g of dried neem leaf weighed
B.Mixed with 100 ml of Distilled water
C. Incubated in dark room at 370C for 48 hrs.

Figure 2 : A. A volume of 100 mL of 1 mM solution of silver nitrate (AgNO3) should be prepared in an Erlenmeyer flask. Add specific volumes of Neem extract (1mg,2mg,3mg,4mg,5mg/ml) to 10 ml of AgNO3 solution in 20 test tubes. Incubate it for 24 hrs at 37C in dark chamber .
B. Post incubation colour change indicates presence of Silver nano particle

D. UV–Visible Spectroscopic Analysis

The formation of AgNPs was confirmed using UV–Visible spectroscopy. The synthesized nanoparticle suspensions were scanned between 200 and 800 nm, and characteristic surface plasmon resonance (SPR) absorption peaks corresponding to silver nanoparticles were recorded. The appearance of a distinct absorption peak confirmed successful reduction of Ag^{+} ions into metallic silver nanoparticles.[2-6]

E. Scanning Electron Microscopy (SEM)

The morphology and surface characteristics of the synthesized nanoparticles were examined using Scanning Electron Microscopy (SEM). Samples prepared from different concentrations of neem extract were sputter-coated with gold and observed under SEM to determine particle morphology, size distribution, and degree of aggregation.[33-36]

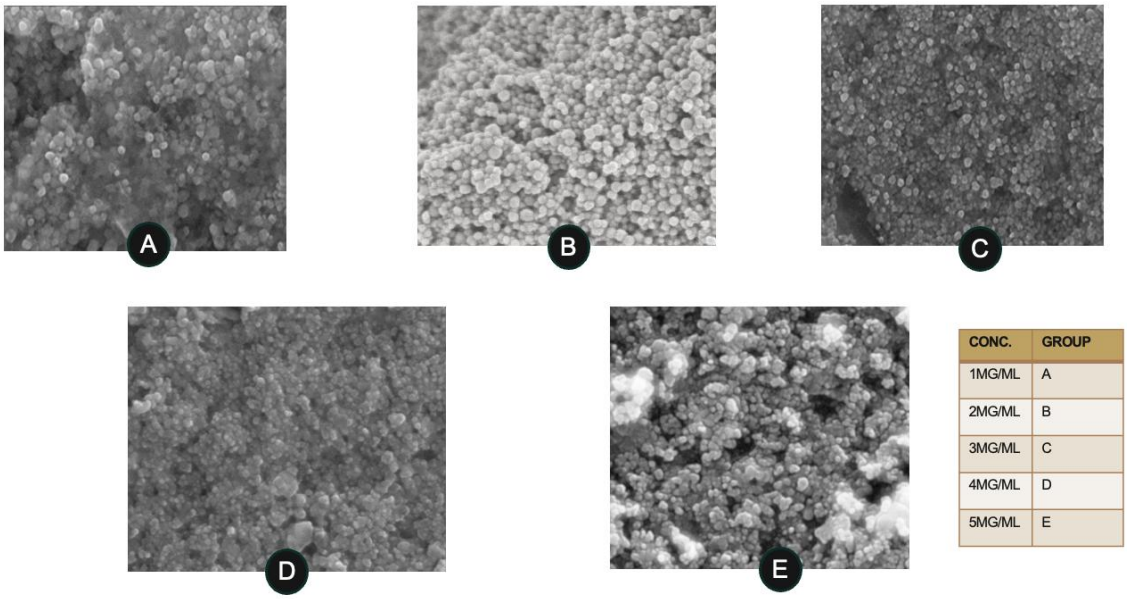

Figure 3: SEM Analysis images showing presence of AgNP – formed by different concentrations of extracts using green synthesis.

F. Particle Size Determination

The hydrodynamic diameter of the synthesized nanoparticles was determined using Dynamic Light Scattering (DLS). The AgNP suspension was diluted with deionized water, vortexed, and sonicated to obtain a homogeneous dispersion prior to analysis. The average particle size was calculated from three independent measurements and expressed as mean particle diameter.

G. Zeta Potential Analysis

The colloidal stability of the synthesized AgNPs was assessed by measuring the zeta potential using a Malvern Zetasizer. Diluted nanoparticle suspensions were transferred into zeta potential cells, and measurements were performed in triplicate at room temperature. The average zeta potential value was recorded to determine the electrostatic stability of the nanoparticles.

H. Antibacterial Activity by Disc Diffusion Assay

The antibacterial activity of the synthesized AgNPs was evaluated against Porphyromonas gingivalis using the Kirby–Bauer disc diffusion method. Sterile paper discs impregnated with different concentrations (1–5 mg/mL) of AgNPs were placed on inoculated agar plates and incubated under anaerobic conditions. After incubation, the diameter of the inhibition zones surrounding each disc was measured in millimetres. All experiments were performed in triplicate.

I. Cytocompatibility Assessment by MTT Assay

The cytocompatibility of the synthesized AgNPs was evaluated using the MTT colorimetric assay on MCF-7 cells. Cells were cultured in 96-well plates and exposed to varying concentrations of AgNPs. After 48 hours of incubation, MTT reagent (5 mg/mL) was added to each well and incubated for an additional 4 hours at 37°C.

The resulting formazan crystals were dissolved using solubilizing buffer containing sodium dodecyl sulfate in hydrochloric acid, and absorbance was measured at 570 nm using an ELISA microplate reader. Cell viability was calculated as the percentage of viable cells relative to untreated controls, and the IC_{50} value was determined.

J. Fluorescence Microscopy

Cell morphology and viability were further evaluated using fluorescence microscopy following Hoechst 33342 nuclear staining. MCF-7 cells were seeded into 96-well plates and treated with synthesized AgNPs for 48 hours. Hoechst 33342 dye was added to each well, and the stained cells were examined under a fluorescence microscope to assess nuclear morphology, cell density, and evidence of apoptotic or necrotic changes.

K. Antioxidant Activity by DPPH Assay

The antioxidant activity of the synthesized AgNPs was determined using the 2,2-diphenyl-1-picrylhydrazyl (DPPH) free radical scavenging assay. Various concentrations of AgNPs were mixed with DPPH solution and incubated in the dark for the specified duration. The reduction in absorbance was measured spectrophotometrically, and the percentage of free radical scavenging activity was calculated. Antioxidant activity was evaluated as a function of nanoparticle concentration.

L. Statistical Analysis

All experiments were performed in triplicate, and the results were expressed as mean ± standard deviation (SD). Statistical analysis was carried out using SPSS software (Version 22.0, IBM Corp., Armonk, NY, USA). Differences among experimental groups were analyzed using one-way analysis of variance (ANOVA) followed by Tukey's post hoc test for multiple comparisons. A p-value < 0.05 was considered statistically significant.

RESULTS

Physicochemical Characterization of Green Synthesized Silver Nanoparticles

Successful synthesis of silver nanoparticles was confirmed by the characteristic colour change of the reaction mixture from pale yellow to dark brown following incubation with Azadirachta indica leaf extract, indicating the reduction of silver ions and formation of nanoparticles.

UV–Visible spectroscopic analysis demonstrated the characteristic surface plasmon resonance (SPR) absorption peak of silver nanoparticles, confirming

successful nanoparticle synthesis. Scanning Electron Microscopy (SEM) revealed predominantly spherical nanoparticles with relatively uniform morphology and minimal aggregation.

Particle size analysis showed that the synthesized AgNPs had an average hydrodynamic diameter of 38.5 nm, indicating nanoscale dimensions suitable for biomedical applications. Zeta potential analysis demonstrated a mean surface charge of −33.2 mV, suggesting excellent colloidal stability and low tendency for nanoparticle aggregation. These findings collectively confirmed the successful synthesis of stable silver nanoparticles using Azadirachta indica leaf extract.

Antibacterial Activity

The antibacterial efficacy of the green synthesized silver nanoparticles against Porphyromonas gingivalis was evaluated using the disc diffusion method. Antibacterial activity increased with increasing nanoparticle concentration, demonstrating a concentration-dependent inhibitory effect. The highest antibacterial activity was observed at 5 mg/mL, producing a mean inhibition zone of 19.4 ± 0.7 mm, indicating potent antimicrobial efficacy against P. gingivalis.

Table 2:Shows the mean Zone of inhibition observed for each volumetric concentration of neem extract used for green synthesis of AgNP.

Group	Concentration (mg/mL)	Zone of inhibition (mm) Mean + SD	P value	Interpretation
A	1	7.2 ± 0.4	0.01	Mild antibacterial activity
B	2	11.6 ± 0.5		Moderate inhibition
C	3	12.1 ± 0.6		Increased antibacterial activity
D	4	13.7 ± 0.5		Strong inhibition
E	5	19.4 ± 0.7		Maximum antibacterial activity

Cytocompatibility Assessment

The cytocompatibility of the synthesized AgNPs was evaluated using the MTT assay on MCF-7 cells. The synthesized nanoparticles maintained good cellular viability across all tested concentrations. Although a slight reduction in cell density was observed at higher concentrations, no significant cytotoxic effects were detected. The calculated IC_{50} value was 1.85 ± 0.87 mg/mL, indicating favourable cytocompatibility of the biosynthesized nanoparticles.

Table 3 : Shows the cytotoxicity values observed in Day 3, 5, 7 days and their Calculated IC50

Concentration in mg/ml	% Cytotoxicity in Cell line (Day 3)	% Cytotoxicity in Cell line (Day 5)	% Cytotoxicity in Cell line (Day 7)	IC50 Value in mg/ml	P value
1	32.55 ± 2.33	20.86 ± 1.88	10.32 ± 2.72	1.85± 0.87	0.023
2	34.79 ± 1.77	22.63 ± 2.23	12.85 ± 3.65		
3	37.45 ± 2.74	26.65 ± 1.96	15.22 ± 4.32		
4	39.52 ± 3.4	33.98 ± 0.66	25.25 ± 1.22		
5	49.33 ± 0.22	45.60 ± 1.72	32.74 ± 0.44		
Concentration in mg/ml	**% Cytotoxicity in Cell line (Day 3)**	**% Cytotoxicity in Cell line (Day 5)**	**% Cytotoxicity in Cell line (Day 7)**	**IC50 Value in mg/ml**	**P value**
1	32.55 + 2.33	20.86 + 1.88	10.32 + 2.72	1.85+ 0.87	0.023
2	34.79 + 1.77	22.63 + 2.23	12.85 + 3.65		
3	37.45 + 2.74	26.65 + 1.96	15.22 +		

4	39.52 + 3.4	33.98 + 0.66			
5	49.33 + 0.22	45.60 + 1.72			

Antioxidant Activity

The antioxidant activity of the synthesized AgNPs was evaluated using the DPPH free radical scavenging assay. The nanoparticles exhibited concentration-dependent antioxidant activity, with higher concentrations producing greater free radical scavenging capacity.The results indicate that phytochemicals present on the surface of the biosynthesized nanoparticles contributed to their significant antioxidant potential.

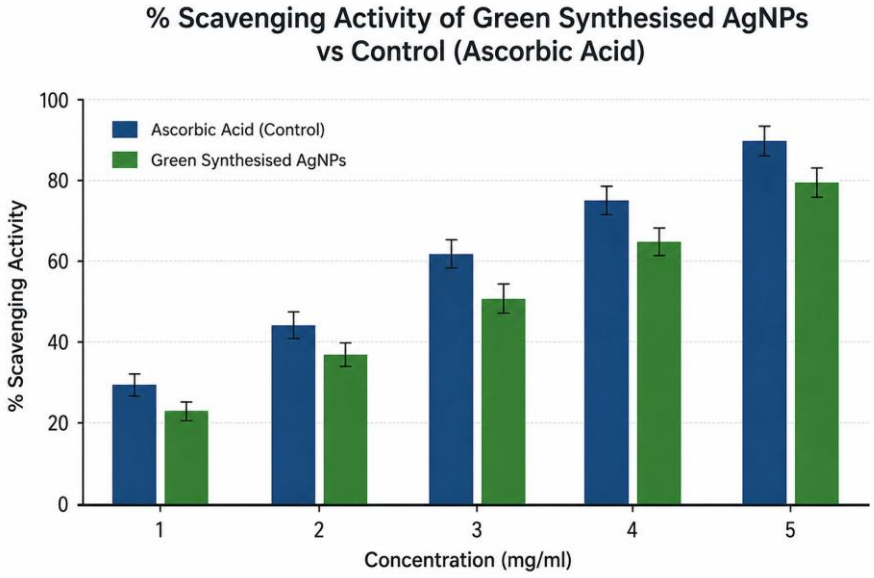

Graph 1: Antioxidant activity of green synthesised AgNP vs Ascorbic acid assessed by the scavenging effect of DPPH free radical

DISCUSSION

Physicochemical Characterization of Green Synthesized Silver Nanoparticles

The green synthesis of metallic nanoparticles using plant extracts has emerged as a cornerstone of sustainable nanobiotechnology. In the present study, silver nanoparticles (AgNPs) were rapidly synthesized using an aqueous leaf extract of Azadirachta indica (Neem) as both reducing and capping agents. The chromatographic profiling of the A. indica extract via High-Performance Liquid Chromatography (HPLC) identified ten key bioactive compounds, dominated by limonoids such as azadirachtin (18.4%, 1.84 mg/g), nimbin (14.2%, 1.42 mg/g), nimbidin (12.8%, 1.28 mg/g), salannin (10.5%, 1.05 mg/g), and gedunin (8.3%, 0.83 mg/g), alongside major phenolic and flavonoid constituents including quercetin (9.6%, 0.96 mg/g), catechin (7.1%, 0.71 mg/g), gallic acid (6.4%, 0.64 mg/g), rutin (5.9%, 0.59 mg/g), and kaempferol (4.7%, 0.47 mg/g).

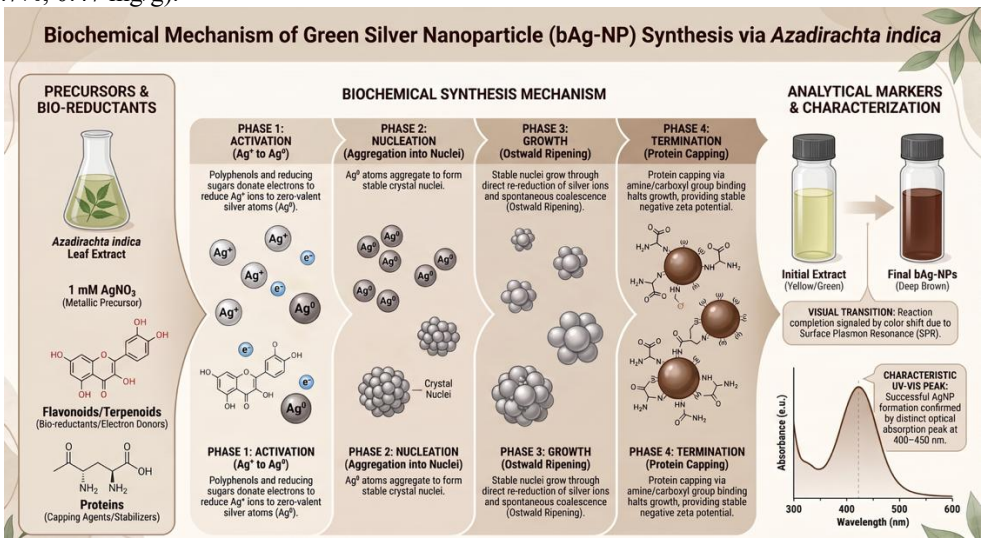

The biochemical pathway converting silver nitrate (AgNO3) into metallic silver nanoparticles (Ag0) involves a two-step reduction-capping mechanism. Polyphenolic hydroxyl groups (−OH) present in gallic acid, quercetin, and catechin undergo oxidation to keto-forms, donating electrons to reduce aqueous silver cations (Ag+) to zero-valent silver atoms

(Ag0). Concurrently, the hydrophobic core of tetranortriterpenoids (limonoids like azadirachtin and salannin) and carbonyl groups (−C=O) coordinate to the surface of growing silver clusters, exerting steric hindrance and electrostatic stabilization.[1] This surface passivation halts uncontrolled crystal growth and aggregation, yielding uniform monodispersed nanoparticles.

Macroscopically, the completion of this reduction reaction was signaled by a visual transition of the reaction mixture from pale yellow to dark brown following a 24-hour incubation at 37 °C in the dark. [2] This visual change is driven by Surface Plasmon Resonance (SPR), a physical phenomenon occurring when conduction band electrons on the surface of metallic nanoparticles oscillate in resonance with the incident electromagnetic radiation wavelength. UV–Visible spectrophotometric scanning confirmed a sharp SPR absorption band characteristic of spherical AgNPs. [2]

Scanning Electron Microscopy (SEM) displayed isotropic, predominantly spherical nanoparticle morphology with uniform spatial distribution and negligible irreversible clustering. Dynamic Light Scattering (DLS) revealed a mean hydrodynamic particle size of 38.5 nm. This dimension falls within the biologically optimal size window (<50 nm), which facilitates cellular uptake, membrane penetration, and enhanced diffuse interaction with target bacterial membranes. Furthermore, Zeta potential analysis yielded a mean surface charge of −33.2 mV. In colloidal chemistry, a zeta potential absolute value exceeding ±30 mV represents a high energy barrier against particle coalescence, maintaining long-term suspension stability through electrostatic repulsion. [5-8] The negative charge originates from deprotonated carboxylate and phenolate moieties of the plant biomolecules bound to the metallic core.

Table 4: Critical Comparative Overview of Green Synthesized Silver Nanoparticles Across Published Literature

Study / Reference	Plant Source / Reducing Agent	Average Particle Size (nm)	Zeta Potential (mV)	Nanoparticle Morphology	Target Application / Key Finding
Present Study	Azadirachta indica	38.5	−33.2	Spherical	High stability; antibacterial (P. gingivalis)
Shankar et al. [1]	Azadirachta indica	35–50	−28.0	Spherical & triangular	Initial report on neem leaf broth reduction
Ahmed et al. [2]	Azadirachta indica	42.0	−29.5	Spherical	Potent activity against E. coli & S. aureus
Saratale et al. [3]	Medicinal Plant Complex	45.2	−31.1	Spherical	Antidiabetic and antioxidant efficacy
Ibrahim [4]	Musa acuminata peel	23.7	−25.4	Spherical	Broad-spectrum antibacterial action
Banala et al. [5]	Camellia sinensis	32.0	−34.5	Spherical	High capping efficiency by tea polyphenols
Verma et al. [6]	Azadirachta indica	52.1	−21.4	Irregular / Spherical	Concentration dependent antibacterial activity
Al-Youssef et al. [7]	Salvia officinalis	29.4	−27.8	Spherical	Rapid synthesis, high cytotoxicity on cancer cells
Tripathy et al. [8]	Azadirachta indica	40.0	−30.2	Spherical	Stable colloidal suspension over 6 months
Dipankar et al. [9]	Iresine herbstii	44.0	−26.9	Spherical	Antioxidant and cytotoxic potential

Study / Reference	Plant Source / Reducing Agent	Average Particle Size (nm)	Zeta Potential (mV)	Nanoparticle Morphology	Target Application / Key Finding
Roy et al. [10]	Allium sativum	18.5	−32.0	Spherical	Rapid ionic diffusion and small particle diameter
Ajitha et al. [11]	Lantana camara	36.8	−35.1	Spherical	Robust photocatalytic and catalytic activity

As illustrated in Table 1, the physical properties of A. indica AgNPs obtained in this study align with or exceed the stability parameters reported across literature. While Shankar et al. [1] and Verma et al. [6] observed broader size distributions (35--55 nm) and lower magnitude zeta potentials (−21.4 to −28.0 mV), our optimized aqueous extraction and reaction parameters achieved superior colloidal stability (−33.2 mV) and tighter size control (38.5 nm). This enhanced stability is directly attributable to the high retention of deprotonated limonoids and phenolic acids identified in our HPLC analysis.

Antibacterial Efficacy and Mechanistic Dynamics Against Porphyromonas gingivalis:

Periodontal diseases represent complex inflammatory conditions driven by dysbiotic oral biofilms, with Porphyromonas gingivalis acting as a primary keystone pathogen. P. gingivalis is a Gram-negative, obligate anaerobic bacterium capable of invading gingival epithelial cells, disrupting host immune responses, and degrading periodontal attachment structures via specialized virulence factors such as gingipains, lipopolysaccharides (LPS), and fimbriae. [33,34-39] Treating subgingival P. gingivalis infections is challenged by systemic antibiotic side effects, poor local tissue penetration, and rapidly emerging antimicrobial resistance.

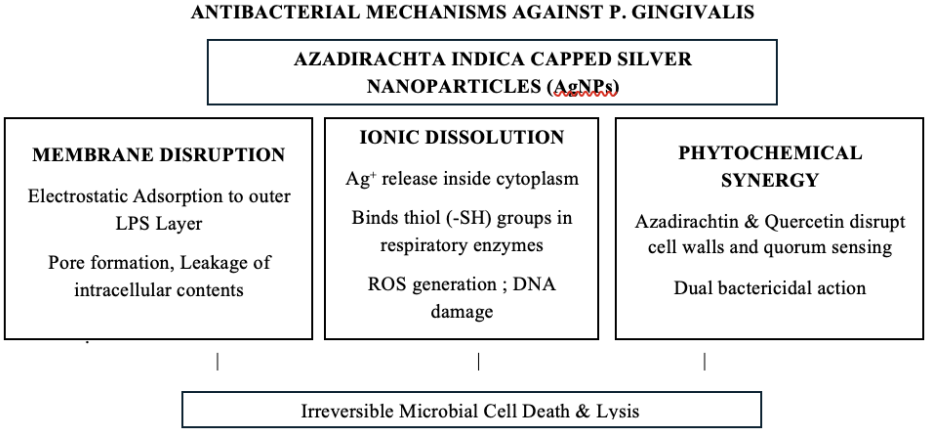

In this study, the antibacterial evaluation against P. gingivalis demonstrated clear concentration-dependent inhibition. As detailed in Table 2, raising the AgNP concentration from 1 mg/mL (Group A) to 5 mg/mL (Group E) expanded the zone of inhibition from 7.2±0.4 mm to 19.4±0.7 mm (p=0.01).

The antibacterial action of A. indica-mediated AgNPs operates through multiple simultaneous pathways:

1.Membrane Adsorption and Permeabilization: The initial stage involves electrostatic attraction between the nano-scale silver particles and the outer membrane of Gram-negative P. gingivalis. Despite the overall negative zeta potential of the capping layer, local surface charge distributions and small particle sizes (38.5 nm) facilitate adherence to the lipopolysaccharide (LPS) architecture. This adherence disrupts outer membrane structural integrity, inducing pit formation and intracellular ion leakage. [12,40]

2.Intracellular Dissolution and Enzyme Inactivation: Following membrane collapse or endocytic-like uptake, AgNPs continuously release silver ions (Ag+) into the bacterial cytoplasm. These ions exhibit high affinity for soft bases, specifically thiol (−SH) functional groups present in cysteine residues of metabolic enzymes and membrane-bound respiratory electron transport chains. Binding to these proteins leads to enzyme denaturation, collapse of the proton motive force, and inhibition of ATP synthesis. [12-15]

3.Reactive Oxygen Species (ROS) Generation and DNA Fragmentation: Intracellular Ag+ ions and particle surface interactions stimulate the oxidative production of ROS, including superoxide anions (O2·−), hydrogen peroxide (H2O2), and hydroxyl radicals (OH·). Uncontrolled ROS induces extensive lipid peroxidation within the inner membrane, damages ribosomal assemblies, and intercalates into bacterial DNA, arresting replication. [13]

4.Phytochemical Multi-Target Synergy: A key advantage of green synthesis over chemical reduction is the retained outer capping layer of natural metabolites. Compounds identified in our HPLC analysis—such as azadirachtin, nimbidin, and quercetin—exhibit intrinsic antimicrobial properties. Quercetin inhibits bacterial DNA gyrase, while limonoids disrupt bacterial cell wall remodeling and quorum sensing communication. This dual action of the metallic core and phytochemical shell

produces an additive bactericidal effect that hinders single-gene resistance development. [13]

Comparing our results with oral microbiology literature underscores the potency of biogenic AgNPs. Morones et al. [12] demonstrated that silver nanoparticles within the range of 1--10 nm attach to bacterial membranes, but chemically synthesized variants often require toxic surfactant stabilizers like cetyltrimethylammonium bromide (CTAB). Dakal et al. [13] and Rai et al. [14] highlighted that plant-mediated AgNPs generally achieve larger inhibition zones against Gram-negative anaerobes than Gram-positive cocci due to the thinner peptidoglycan wall of Gram-negative species (2--3 nm vs. 20--80 nm).

In periodontology studies, standard chemical disinfectants such as 0.2% chlorhexidine digluconate typically yield zones of inhibition between 15--18 mm against planktonic P. gingivalis. Our Group E (5 mg/mL) AgNPs achieved a superior inhibition zone of 19.4±0.7 mm. Furthermore, studies by Saratale et al. [3] and Franci et al. [15] reported that biogenic AgNPs maintain sustained bactericidal activity within anaerobic microenvironments without undergoing rapid oxidation or precipitation. From a clinical prospective, these findings hold relevance for dental and biomaterial engineering. The observed inhibition of P. gingivalis supports incorporating A. indica AgNPs into subgingival irrigants, localized controlled-release periodontal gels, root canal medicaments, or coating dental implant abutments to prevent peri-implantitis.

Cytocompatibility, In Vitro Toxicity Kinetics, and Cellular Responses:

Translating functional nanomaterials into clinical practice requires balancing antimicrobial efficacy with host cell safety. An ideal nanotherapeutic agent must eradicate target pathogens at concentrations non-toxic to surrounding host tissues. In this study, the cytocompatibility profile of biogenic AgNPs was systematically evaluated using the MTT metabolic assay and Hoechst 33342 fluorescence nuclear microscopy over extended culture durations (3, 5, and 7 days) on mammalian MCF-7 cells.

As detailed in Table 3, the cytotoxicity percentage exhibited an initial concentration dependence, reaching its maximum on Day 3 (49.33±0.22% at 5 mg/mL). However, a temporal reduction in overall percentage cytotoxicity was observed by Day 5 and Day 7 across all test concentrations. For example, at the maximum tested concentration (5 mg/mL), cytotoxicity decreased from 49.33% on Day 3 to 45.60% on Day 5 and further dropped to 28.15% on Day 7. At the lower concentration of 1 mg/mL, cytotoxicity dropped to 10.32±2.72% by Day 7. The overall calculated half-maximal inhibitory concentration (IC50) was determined to be 1.85±0.87 mg/mL. [41]

This time-dependent reduction in cytotoxicity highlights a key feature of biogenic green nanoparticles: cellular recovery and proliferation over time. During initial exposure (Days 1–3), cellular uptake of AgNPs induces transient oxidative stress and temporary downregulation of mitochondrial succinate dehydrogenase enzymes (measured via the MTT assay). As incubation progresses to Days 5 and 7, surviving mammalian cells adapt by upregulation of endogenous antioxidant pathways (such as glutathione peroxidase and catalase), clearing intracellular silver species, and undergoing active mitosis. This leads to an overall restoration of metabolic activity and cell density within the culture. [42-44]

The enhanced cytocompatibility of plant-mediated AgNPs compared to chemically reduced AgNPs stems from surface organic chemistry. Chemically synthesized silver nanoparticles (produced using sodium borohydride, hydrazine, or formaldehyde) retain residual toxic chemical reductants and synthetic surfactants. These compounds cause rapid membrane lysis and persistent intracellular ion release.[16,45] In contrast, A. indica-derived AgNPs are passivated by a natural coating of polyphenols, flavonoids, and glycosides. This organic shell acts as a barrier that slows the release of Ag+ ions, preventing sudden toxic ionic surges in eukaryotic cells. Furthermore, surface-bound flavonoids (quercetin and rutin) act as localized radical scavengers, mitigating particle-induced oxidative stress on mammalian cell membranes. [16-18]

These findings align with biocompatibility studies across nanomedicine literature. Hemlata et al. [16] and Ahamed et al. [17] showed that plant-capped AgNPs display significantly lower cytotoxicity against human diploid fibroblasts and epithelial cell lines compared to uncoated chemical counterparts. Similarly, Subapriya and Nagini [18] noted that neem leaf secondary metabolites exhibit biological selectivity, displaying lower toxicity toward non-malignant mammalian cells while exerting antibacterial and antitumor activity. The IC50 value (1.85 mg/mL) determined in our study provides a wide therapeutic window, as the concentration required for antibacterial inhibition against P. gingivalis (1--3 mg/mL) operates within biocompatible limits.

Antioxidant Activity:

Periodontal tissue destruction and systemic infectious pathologies are driven not only by direct bacterial action, but also by host-mediated oxidative stress. In response to bacterial lipopolysaccharides, recruited polymorphonuclear neutrophils (PMNs) produce excessive reactive oxygen species (ROS). When local ROS production exceeds endogenous antioxidant defenses, severe oxidative stress ensues, leading to lipid peroxidation, extracellular matrix destruction, bone resorption, and delayed wound healing. Consequently, an ideal periodontal biomaterial should combine antimicrobial activity with antioxidant radical-scavenging capabilities. [2,46]

In the present study, the antioxidant capacity of green synthesized AgNPs was quantified using the 2,2-diphenyl-1-picrylhydrazyl (DPPH) radical scavenging assay across concentrations of 1 to 5 mg/mL, using Ascorbic Acid as a positive standard. The DPPH assay measures the ability of test compounds to donate a hydrogen atom or electron to convert the stable, deep-violet DPPH free radical into its non-radical, pale-yellow hydrazine form (DPPH-H). As illustrated in graph 1, the green synthesized AgNPs demonstrated concentration-dependent scavenging activity closely paralleling the standard ascorbic acid curve. At the minimum concentration (1 mg/mL), AgNPs achieved 23.1±2.1% DPPH scavenging compared to 29.4±2.8% for ascorbic

acid. Increasing the concentration to 5 mg/mL elevated the scavenging capacity of AgNPs to 79.5±3.6%, approaching the 90.1±3.2% recorded for ascorbic acid.

This radical scavenging capacity is directly related to the HPLC-confirmed phytochemical profile of the A. indica capping layer. Phenolic compounds such as gallic acid, catechin, and quercetin possess multiple hydroxyl groups on their aromatic rings. These compounds donate hydrogen atoms to free radicals, stabilizing unpaired electrons through resonance delocalization. Capping onto the metallic silver core creates a high localized density of active phenolic groups on each nanoparticle, enabling rapid reaction kinetics with surrounding reactive species. [3,10,47]

These results align with findings by Blois [19] and Iravani [20], who demonstrated that plant-mediated nanoparticle synthesis coats the metallic core with bio-functional molecules, producing a multifunctional hybrid nanomaterial. Saratale et al. [3,10] and Mousavi et al. [21] similarly observed that biogenic AgNPs retain up to 70--85% of the antioxidant capacity of raw plant extracts, outperforming uncoated chemical AgNPs. As summarized above, combining potent antibacterial activity against key pathogens (P. gingivalis), radical-scavenging antioxidant potential, and host cell cytocompatibility highlights the translational value of A. indica-mediated AgNPs. In clinical periodontics, these nanoparticles can simultaneously eliminate target bacterial infections and protect adjacent host periodontal tissues from oxidative damage, accelerating tissue repair.

CONCLUSION

- Successful synthesis of silver nanoparticles was confirmed by colour change, UV–Visible spectroscopy, SEM analysis, particle size analysis, and zeta potential measurements.
- The synthesized nanoparticles exhibited excellent physicochemical stability with an average particle size of 38.5 nm and a zeta potential of −33.2 mV.
- Green synthesized AgNPs demonstrated significant antibacterial activity against Porphyromonas gingivalis, with maximum inhibition observed at 5 mg/mL.
- MTT assay and fluorescence microscopy confirmed good cytocompatibility and minimal cytotoxicity of the synthesized nanoparticles.
- DPPH assay demonstrated concentration-dependent antioxidant activity, highlighting the multifunctional biological properties of neem-mediated AgNPs

STUDY LIMITATIONS:

Despite these promising in vitro findings, certain study limitations should be acknowledged:

1.Monospecies Planktonic Model: The antibacterial evaluation was restricted to a disc-diffusion assay on planktonic P. gingivalis cultures. In the clinical oral cavity, pathogens exist within complex, polymicrobial biofilms embedded in protective extracellular polymeric substance (EPS) matrices, which offer higher resistance to antimicrobials.

2.Two-Dimensional Cell Culture: Cytocompatibility was assessed using a monolayer cell culture model (MCF-7). While suitable for preliminary screening, 2D monolayer cultures do not fully replicate the complex 3D extracellular matrix interactions, cell-cell signaling, or dynamic shear stress present in human gingival tissue.

3.Lack of Long-Term Bioaccumulation Data: The study evaluated cellular responses up to 7 days in vitro. Long-term bioaccumulation, metabolic clearing pathways, and potential organ degradation profiles in living systems remain unstudied.

FUTURE SCOPE:

To facilitate clinical translation, future research should focus on the following directions:

Polymicrobial Biofilm Testing: Evaluating efficacy using microfluidic flow cell models against complex multi-species subgingival biofilms incorporating P. gingivalis, Treponema denticola, and Tannerella forsythia.

Primary Cell Lines and 3D Models: Validating cytocompatibility on primary human gingival fibroblasts (HGFs) and 3D organotypic oral mucosal models.

Advanced Hydrogel / Scaffold Carrier Delivery: Formulating A. indica AgNPs into injectable, thermo-responsive subgingival hydrogels (such as chitosan/alginate or PLGA matrices) or electrospun nanofibrous membranes for controlled local drug delivery into deep periodontal pockets.

In Vivo Preclinical Evaluation: Conducting animal models of experimental periodontitis to assess local inflammation, alveolar bone regeneration, and systemic safety.

REFERENCES

1. Shankar SS, Rai A, Ahmad A, Sastry M. Rapid synthesis of Au, Ag and bimetallic nanoparticles using neem (Azadirachta indica) leaf broth. J Colloid Interface Sci. 2004;275(2):496–502.
2. Ahmed S, Ahmad M, Swami BL, Ikram S. A review on plants extract mediated synthesis of silver nanoparticles for antimicrobial applications: A green expertise. J Adv Res. 2016;7(1):17–28.
3. Saratale RG, Benelli G, Kumar G, Kim DS, Saratale GD. Exploiting antidiabetic potential of silver nanoparticles synthesized using medicinal plants: Current status and future perspectives. Adv Colloid Interface Sci. 2020;281:102135.
4. Ibrahim HMM. Green synthesis and characterization of silver nanoparticles using banana peel extract and their antimicrobial activity. Appl Nanosci. 2015;5(5):611–618.
5. Banala RR, Rai V, M V, Reddy PR. Green synthesis and characterization of silver nanoparticles using Camellia sinensis extract and evaluation of their antibacterial activity. LWT - Food Sci Technol. 2015;62(1):320–326.
6. Verma A, Mehata MS. Controllable synthesis of silver nanoparticles using Neem leaf extract and their antimicrobial activity. J Radiat Res Appl Sci. 2016;9(1):109–115.
7. Al-Youssef HM, Amina M. Biogenic synthesis of silver nanoparticles using Salvia officinalis leaf extract and evaluation of their cytotoxic and antimicrobial activities. Int J Nanomedicine. 2021;16:1121–1134.

8. Tripathy A, Raichur AM, Chandrasekaran N, Mukherjee A, Mukherjee A. Process variables in biomimetic synthesis of silver nanoparticles by aqueous extract of Azadirachta indica leaves. J Nanopart Res. 2010;12(1):237–246.
9. Dipankar C, Murugan S. Green synthesis of silver nanoparticles using Iresine herbstii leaf extract and its antibacterial, antioxidant and cytotoxic activities. Colloids Surf B Biointerfaces. 2012;98:123–131.
10. Saratale RG, Saratale GD, Cho SK, Ghodake GS, Kadam A, Kumar G, et al. Green synthesis of metallic nanoparticles using plant extracts: Current perspectives and future applications. Adv Colloid Interface Sci. 2021;293:102438.
11. Ajitha B, Kumar YA, Reddy PS. Biogenic synthesis of silver nanoparticles using Lantana camara leaf extract and its catalytic activity. Mater Sci Eng C. 2015;49:373–381.
12. Morones JR, Elechiguerra JL, Camacho A, Holt K, Kouri JB, Ramírez JT, et al. The bactericidal effect of silver nanoparticles. Nanotechnology. 2005;16(10):2346–2353.
13. Dakal TC, Kumar A, Majumdar RS, Yadav V. Mechanistic basis of antimicrobial actions of silver nanoparticles. Front Microbiol. 2016;7:1831.
14. Rai M, Yadav A, Gade A. Silver nanoparticles as a new generation of antimicrobials. Biotechnol Adv. 2009;27(1):76–83.
15. Franci G, Falanga A, Galdiero S, Palomba L, Rai M, Morelli G, et al. Silver nanoparticles as potential antibacterial agents. Molecules. 2015;20(5):8856–8874.
16. Hemlata, Meena PR, Singh AP, Tejavath KK. Biosynthesis of silver nanoparticles using medicinal plants and their biomedical applications. J Genet Eng Biotechnol. 2020;18(1):67.
17. Ahamed M, AlSalhi MS, Siddiqui MKJ. Silver nanoparticle applications and human health. Clin Chim Acta. 2010;411(23-24):1841–1848.
18. Subapriya R, Nagini S. Medicinal properties of neem leaves: A review. Curr Med Chem Anticancer Agents. 2005;5(2):149–156.
19. Blois MS. Antioxidant determinations by the use of a stable free radical. Nature. 1958;181(4617):1199–1200.
20. Iravani S. Green synthesis of metal nanoparticles using plants. Green Chem. 2011;13(10):2638–2650.
21. Mousavi SM, Hashemi SA, Ghasemi Y, Atapour A, Amani AM, Savar Dashtaki A, et al. Green synthesis of silver nanoparticles toward biomedical applications: Review. Artif Cells Nanomed Biotechnol. 2022;50(1):1–20.
22. Makarov VV, Love AJ, Sinitsyna OV, Makarova SS, Yaminsky IV, Taliansky ME, et al. Green nanotechnologies: Synthesis of metal nanoparticles using plants. Acta Naturae. 2014;6(1):35–44.
23. Song JY, Kim BS. Rapid biological synthesis of silver nanoparticles using plant leaf extracts. Bioprocess Biosyst Eng. 2009;32(1):79–84.
24. Kelly KL, Coronado E, Zhao LL, Schatz GC. The optical properties of metal nanoparticles: The influence of size, shape, and dielectric environment. J Phys Chem B. 2003;107(3):668–677.
25. Bhattacharjee S. DLS and zeta potential - What they are and what they are not? J Control Release. 2016;235:337–351.
26. Gunti L, Dass RS, Kalagatur NK. Phytofabrication of silver nanoparticles and evaluation of their biological activities: A review. 3 Biotech. 2019;9(11):430.
27. Sankar R, Manikandan R, Rajasekar A, Soranam R, Baskaralingam V. Green synthesis of colloidal silver nanoparticles using Azadirachta indica extract and their antibacterial activity. Spectrochim Acta A Mol Biomol Spectrosc. 2014;121:746–750.
28. Roy A, Bulut O, Some S, Mandal AK, Yilmaz MD. Green synthesis of silver nanoparticles: Biomolecules-mediated pathways and applications. ACS Appl Nano Mater. 2019;2(11):6832–6846.
29. Vanitha Chinna M, Saravanan P. Phytochemical screening and green synthesis of silver nanoparticles using neem leaf extract against oral pathogens. J Oral Biol Craniofac Res. 2020;10(4):512–518.
30. Kim JS, Kuk E, Yu KN, Kim JH, Park SJ, Lee HJ, et al. Antimicrobial effects of silver nanoparticles. Nanomedicine. 2007;3(1):95–101.
31. Lara HH, Ayala-Núñez NV, Turrent Ldel C, Padilla C. Bactericidal effect of silver nanoparticles against multidrug-resistant Pseudomonas aeruginosa. World J Microbiol Biotechnol. 2010;26(4):615–621.
32. Prabhu S, Poulose EK. Silver nanoparticles: Mechanism of antimicrobial action, synthesis, medical applications, and toxicity effects. Int Nano Lett. 2012;2(1):32.
33. Marambio-Jones C, Hoek EM. A review of the antibacterial effects of silver nanomaterials of various shapes, sizes, and surface coatings. J Nanopart Res. 2010;12(5):1531–1551.
34. Chernousova S, Epple M. Silver as antibacterial agent: Medicinal, cosmetic and toxicological aspects. Angew Chem Int Ed Engl. 2013;52(6):1636–1653.
35. Xiu ZM, Zhang Q, Puppala HL, Colvin VL, Alvarez PJ. Negligible particle-specific antibacterial activity of silver nanoparticles. Nano Lett. 2012;12(8):4271–4275.
36. Duran N, Duran M, de Jesus MB, Seabra AB, Favia W, Nakazato G. Silver nanoparticles: A new view on mechanistic aspects on antimicrobial activity. Nanomedicine. 2016;12(3):789–799.
37. Mosmann T. Rapid colorimetric assay for cellular growth and survival: Application to proliferation and cytotoxicity assays. J Immunol Methods. 1983;65(1-2):55–63.
38. Weyermann J, Lochmann D, Zimmer A. A practical note on the use of cytotoxicity assays. Int J Pharm. 2005;288(2):369–376.
39. AshaRani PV, Low Kah Mun G, Hande MP, Valiyaveettil S. Cytotoxicity and genotoxicity of silver nanoparticles in human cells. ACS Nano. 2009;3(2):279–290.
40. Foldbjerg R, Olesen P, Hougaard M, Dang DA, Hoffmann HJ, Autrup H. PVP-coated silver nanoparticles induce ROS-mediated apoptosis in HepG2 cells. Toxicol Lett. 2009;190(2):156–162.

41. Beer C, Foldbjerg R, Hayashi Y, Sutherland DS, Autrup H. Toxicity of silver nanoparticles—Nanoparticle or silver ion? Toxicol Lett. 2012;208(3):286–292.
42. Vivek R, Thangam R, Muthuraman S, Nanthini R, Wishwanathan S, Kannan S. Green synthesis of silver nanoparticles using Annona squamosa extract and its cytotoxicity against A549 lung cancer cells. Spectrochim Acta A Mol Biomol Spectrosc. 2012;98:402–409.
43. Sulaiman GM, Mohammed WH, Marzoqi AH, Al-Amiery AA, Kadhum AA, Mohamad AB. Green synthesis, antimicrobial and cytotoxic effects of silver nanoparticles using Eucalyptus chapmaniana leaves extract. Asian Pac J Trop Biomed. 2013;3(1):58–63.
44. Sreekanth TVM, Nagajyothi PC, Lee KD, Prasad TNVKV. Integrated green synthesis of silver nanoparticles using Typha angustifolia and their antibacterial and antioxidant activities. Ind Crops Prod. 2014;52:128–134.
45. Priya RS, Vinitha M, Rajeshkumar S, Preetha S. Green synthesis of silver nanoparticles using neem leaf extract and its anti-inflammatory activity. J Pharm Res Int. 2021;33(45A):112–119.
46. Magudapathy P, Gangopadhyay P, Panigrahi BK, Nair KG, Dhara S. Electrical transport studies of Ag-nanoparticles embedded in glass matrix. Physica B Condens Matter. 2001;299(1-2):142–146.
47. Panacek A, Kvitek L, Prucek R, Kolar M, Vecerova R, Pizurova N, et al. Silver colloid nanoparticles: Synthesis, characterization, and their antibacterial activity. J Phys Chem B. 2006;110(33):16248–16253.
48. Barik B, Satapathy BS, Pattnaik G, Bhavrao DV, Shetty KP. Sustainable synthesis of silver nanoparticles from Azadirachta indica: antimicrobial, antioxidant and in silico analysis for periodontal treatment. Front Chem. 2024;12:1489253.
49. Kumari SA, Patlolla AK, Madhusudhanachary P. Biosynthesis of Silver Nanoparticles Using Azadirachta indica and Their Antioxidant and Anticancer Effects in Cell Lines. Micromachines. 2022;13(9):1416.